Available online at www.sciencedirect.com
ScienceDirect
Journal of Photochemistry and Photobiology A: Chemistry 197 (2008) 364–374
Journal of Photochemistry and Photobiology A:Chemistry
www.elsevier.com/locate/jphotochem

Solvent dependence of the charge-transfer properties of a quaterthiophene–anthraquinone dyad

Jiandi Wan [a,b,1], Amy Ferreira [a], Wei Xia [a,2], Chak Him Chow [b,3], Kensuke Takechi [c], Prashant V. Kamat [c], Guilford Jones II [b], Valentine I. Vullev [a,*]

[a] *Department of Bioengineering, University of California, Riverside, CA 92521, United States*
[b] *Department of Chemistry and Photonics Center, Boston University, Boston, MA 02215, United States*
[c] *Radiation Laboratory, Departments of Chemistry and Biochemistry and Chemical and Biomolecular Engineering, University of Notre Dame, IN 46556, United States*

Received 22 October 2007; received in revised form 8 January 2008; accepted 29 January 2008
Available online 8 February 2008

Abstract

An electron donor–acceptor dyad (quaterthiophene–anthraquinone) mediates ultrafast intramolecular photoinduced charge separation and consequent charge recombination when in polar or moderately polar solvents. Alternatively, non-polar media completely impedes the initial photoinduced electron transfer by causing enough destabilization of the charge-transfer state and shifting its energy above the energy of the lowest locally excited singlet state. Furthermore, femtosecond transient-absorption spectroscopy reveals that for the solvents mediating the initial photoinduced electron-transfer process, the charge recombination rates were slower than the rates of charge separation. This behavior of donor–acceptor systems is essential for solar-energy-conversion applications. For the donor–acceptor dyad described in this study, the electron-transfer driving force and reorganization energy place the charge-recombination processes in the Marcus inverted region.

Keywords: Oligothiophene; Quinone; Electron transfer; Charge separation; Charge recombination; Fluorescence quenching; Laser flash photolysis; Charge-transfer rate; Rehm weller equation; Born equation

1. Introduction

This article describes the dependence of the electron-transfer properties of a donor–acceptor dyad on solvent polarity. Alterations of the polarity of the media shift the energy of the charge-separated state leading to changes in the observed electron-transfer kinetics.

For solar-energy-conversion applications, it is essential to employ systems that, upon photoexcitation, generate long-lived charge-transfer (CT) states. Therefore, electron donor–acceptor conjugates, which mediate fast photoinduced charge transfer and slow consequent back charge transfer, possess features that prove useful for light-harvesting applications [1]. Triplet formation, [1–5] local electric fields [6–11] and increased media viscosity [12–14] present venues for generating long-lived CT species.

For minimal losses during light-energy conversion, the energy gaps between the CT and the lowest locally excited states of the selected donor–acceptor systems are smaller than the energy gaps between the ground and the CT states. Therefore, in comparison with the back CT, the photoinduced charge transfer processes are expected to be faster at smaller driving forces. Adopting the semiclassical terminology, [15] the reorganization energy of the system, λ, should ideally be comparable to the driving force of the photoinduced charge transfer, i.e., $\lambda \approx -\Delta G_{ct}^{(0)}$, [16] placing the forward CT processes near the tip of the Marcus curve and the back CT – in the inverted region.

Excessively large driving forces for the back charge transfer (exceeding 2.5 eV, for example) may place the back CT processes in the double-inverted region [17–19]. No experimental

* Corresponding author. Tel.: +1 951 827 6239; fax: +1 951 827 6416.
E-mail address: vullev@ucr.edu (V.I. Vullev).
[1] Present address: Division of Engineering and Applied Sciences, Harvard University, 29 Oxford Str., Cambridge, MA 02138, United States.
[2] Present address: Department of Chemical Engineering, University of Rochester, Rochester, NY 14627, United States.
[3] Present address: Department of Chemistry, Tufts University, Medford, MA 02155, United States.

1010-6030/$ – see front matter © 2008 Elsevier B.V. All rights reserved.
doi:10.1016/j.jphotochem.2008.01.016

evidence, however, is yet available for systems that manifest forward CT occurring in a regime near the tip of the Marcus curve with rate constants equal to or smaller than the rate constants for the corresponding back CT processes occurring in the double-inverted region.

Due to their electronic and optical properties, thiophene oligomers received substantial attention as potential materials for photovoltaic and electroluminescence applications [20–29]. Oligothiophenes modified with electron donating or the electron withdrawing groups exhibited superior hole-transport or electron-transport properties [28]. Among the polymer photovoltaic devices, solar cells based on polythiophenes manifest some of the highest power conversion efficiencies [30–32]. This engineering success, as well as the growing demands for organic electronic materials, has been the driving force behind the increasing interest in thiophene-containing electron-donor–acceptor dyads or donor-bridge-acceptor triads that mediate photoinduced charge separation [33–42].

The dependence of the charge-transfer rates on the polarity of the media [1,43–46] presents an approach for tuning the CT kinetics. Usually, decrease in the solvent polarity results not only in destabilization of charge-separation states, but also in a decrease in the outer reorganization energy.

Utilizing an oligothiophene derivative, dihexylquaterthiophene (T4), as an electron donor and a principal chromophore, we prepared a charge-transfer dyad and investigated the dependence of its properties on the media polarity. While T4 is a short enough oligomer to be treated as a single chromophore, [35,47] quaterthiophenes are long enough to exhibit photophysical properties comparable with the properties of the polythiophenes [48].

For this study, we selected an electron acceptor with intermediate strength, anthraquinone (AQ), that for moderately polar solvents provides sufficient driving force for fast photoinduced charge separation (CS) and allows for considerably larger driving force for the consequent charge recombination (CR).

The fluorescence and transient-absorption properties of the T4–AQ dyad revealed that non-polar solvents suppress photoinduced charge separation. For polar and moderately polar solvent media, however, photoexcitation of T4 initiates intramolecular electron-transfer, i.e., CS occurring in the picosecond and subpicosecond time regime, followed by slower CR. For the investigated solvents, the electron-transfer driving force for CS is smaller than the driving force for CR, indicating that the back electron-transfer processes occur in the Marcus inverted region.

2. Experimental

2.1. Materials

The 3-hexylthiophene, *N*-bromosuccinimide (NBS), iodomethane, 2,5-dibromobithiophene, [1,3-bis(diphenylphosphino)propane]-dichloronickel(II) chloride ($Ni(dppp)Cl_2$), 1.6 M *n*-butyllithium solution (LiBu), thionyl chloride, 2-aminoanthraquinone (aAQ), pyridine, dry tetrahydrofuran and dry dichloromethane were purchased from Aldrich. Tetrachloromethane (CCl_4), chloroform ($CHCl_3$), dichloromethane (CH_2Cl_2), dimethylsulfoxide (DMSO), *n*-hexane, toluene, ethylacetate (EtAc), tetrahydrofuran (THF), acetone and acetonitrile (MeCN), spectroscopic grade or *Omnisolve* were purchased from Aldrich, Fisher or VWR and used as received. The 2-aminoanthraquinone was recrystallized in ethanol before use. All reactions were run in oven-dried glassware under an atmosphere of argon. Silica gel (40 μm, 230–400 mesh, Baker) was employed as the stationary phase for column chromatography. Samples were loaded into the columns as solutions in minimal amount of CH_2Cl_2 or acetone/CH_2Cl_2 and eluted with concentration gradients of hexanes, CH_2Cl_2 and acetone up to the reported percentage. High-resolution mass spectra (HMRS) were obtained with a Finnegan MAT90 spectrometer. NMR spectra were collected with a Varian 400 spectrometer.

2-Bromo 3-hexylthiophene (**1**) [49]. 3-hexylthiophene (20 g, 0.119 mol) was dissolved in DMF (105 mL) in a 500-mL round bottom flask wrapped with aluminum foil and stirred for 5 min. In an aluminum foil-wrapped 200-mL round bottom flask, NBS (22 g, 0.126 mol) was dissolved in DMF (110 mL) and stirred for 5 min. The NBS solution was transferred to the 3-hexylthiophene solution drop-wise over a period of 30 min. The reaction mixture produced heat during the process. The mixture was stirred at room temperature for 40 h and then poured over ice in a beaker. Light yellow oil was deposited at the bottom of the beaker. The oil was collected and extracted five times with 20 mL ether. The organic phases were combined, washed with 50 mL water and dried over sodium sulfate. Evaporation of the solvent and distillation under reduced pressure (b.p. 136–137 °C/10^{-2} mm Hg) yielded **1** as light yellow oil (21.35 g, 73%). ^{1}H NMR (400 MHz, $CDCl_3$) δ ppm 7.19 (d, J = 5.2 Hz, 1H), 6.79 (d, J = 5.2 Hz, 1H), 2.59 (t, J = 8 Hz, 2H), 1.59 (m, 2H), 1.33 (m, 6H), 0.88 (m, 3H).

(3,3′-*dihexyl*)-2,2′:5′,2″:5″,2‴ *quaterthiophene* (**2**) [33]. In order to prepare a Grignard reagent, an oven-dried 500-mL three-neck flask was charged with magnesium (1.2 g, 0.05 mol), dry ether (100 mL) and iodine (0.10 g, 0.39 mmol). The mixture was stirred for 30 min. Iodomethane (0.10 mL, 1.6 mmol) was added. The mixture was stirred again until the mixture turned white. Solution of **1** (10 g, 0.04 mol) in dry ether (25 mL) was added drop-wise over a period of 30 min. The mixture was heated under reflux for 2 h. In another oven-dried 250-mL round bottom flask, 2,5-dibromobithiophene (5.0 g, 0.015 mol), $Ni(dppp)Cl_2$ (0.05 g), and ether (100 mL) were mixed with stirring. The Grignard reagent was transferred to the dibromobithiophene solution slowly. The mixture was reddish brown and turned darker as more Grignard reagent was added. The reaction mixture was heated under reflux for 20 h and then washed with 1M HCl solution (50 mL) that was neutralized with 0.5 N sodium bicarbonate solution (100 mL) and washed again with water. The crude product was extracted with dichloromethane and dried over sodium sulfate. This crude product, which showed two components on TLC, was purified by column chromatography (silica gel, hexane) to yield **2** as brown oil (5.21 g, 68%). ^{1}H NMR (400 MHz, acetone-d_6) δ ppm 7.37 (d, J = 5.2 Hz, 2H), 7.27 (d, J = 3.6 Hz, 2H), 7.11 (d, J = 4.0 Hz, 2H), 7.03 (d, J = 5.6 Hz,

2H), 2.80 (t, J = 6.8 Hz, 4H), 1.65 (m, 4H), 1.34 (m, 12H), 0.86 (m, 6H).

(3,3′-*dihexyl*)-2,2′:5′,2″:5″,2‴ *quaterthiophene-5-carboxylic acid* (**T4a**) [50–52]. A solution of **2** (4.8 g, 0.01 mol) in dry THF (200 mL) was stirred in an acetone/dry ice bath (−78 °C) for 30 min. 1.6 M *n*-BuLi in hexane (5.5 mL, 0.008 mol) was added slowly. The mixture was stirred in the acetone/dry ice bath (−78 °C) for one additional hour. When LiBu was added, the color of the solution changed from yellow to reddish yellow. Dry carbon dioxide was introduced to the mixture until saturation. As carbon dioxide was dissolved, the mixture turned orange. The mixture was stirred for three hours in the acetone/dry ice bath (−78 °C) and overnight at room temperature. The solution was carefully neutralized with 1 M HCl (50 mL) A small amount of orange precipitate formed when HCl was initially added but the precipitate re-dissolved upon the completion of the addition of the HCl solution. Ethyl acetate was added to the solution. The organic phase was collected, washed with 1 M HCl (50 mL) and water (200 mL), dried over magnesium sulfate, and concentrated to dryness. The residue, which was a reddish orange solid, was column chromatographed (silica gel; 10% acetone/CH_2Cl_2) to yield **3** (2.5 g, 50%) of an orange solid. m.p. 99–100 °C. ^{1}H NMR (400 MHz, acetone-d_6) δ ppm: 7.69 (s, 1H), 7.41 (d, J = 4.8 Hz, 1H), 7.36 (t, J = 3.2 Hz, 2H), 7.31 (d, J = 5.6 Hz, 1H), 7.16 (d, J = 4.0 Hz, 1H), 7.06 (d, J = 4.8 Hz, 1H), 2.84 (t, J = 6.8 Hz, 4H), 1.69 (m, 4H), 1.34 (m, 12H), 0.88 (m, 6H). HRMS (CI, 70 ev) *m/z*: [M^+] 542.1437 g mol^{-1} e^{-1}; calculated: 542.319 g/mol ($C_{29}H_{34}O_2S_4$).

2-((3,3′-*dihexyl*)-2,2′:5′,2″:5″,2‴ *quaterthiophene)-anthraquinone* (**T4–AQ**). A 97% solution of $SOCl_2$ (20 mL) was distilled (b.p. 77 °C) and added to **3** (0.87 g; 0.0016 mol). The dark brown mixture was heated under reflux for 90 min. A blackish solution was seen towards the end of the reflux. The solvent was then removed by rotary evaporation and the residue was washed with 3 mL × 5 mL portions of dry dichloromethane, which was then evaporated. A black gel-like substance was observed when the solvent was evaporated. The black gel was re-dissolved in dry toluene (20 mL). A few drops of pyridine and 2-aminoanthraquinone (0.75 g; 0.0034 mol) were introduced into the solution. The dark brown mixture was stirred in an ice-bath for 10 min and then heated under reflux for 24 h. The solvent was evaporated by a rotary evaporator to yield a dark reddish brown residue. The residue was dissolved in 25 mL CH_2Cl_2 and washed with 0.5 M sodium carbonate (100 mL). The solution was dried over sodium sulfate. Purification by column chromatography (silica gel; 100% CH_2Cl_2) yielded crude **T4–AQ** as a brown solid. The crude product was recrystallized in ethanol with 40% CH_2Cl_2 to yield **T4–AQ** (0.24 g, 20%). ^{1}H NMR (400 MHz, $CDCl_3$) δ ppm 8.42 (m, 1H), 8.31 (m, 4H), 8.19 (s, 1H), 8.11 (m, 1H), 7.75 (m, 3H), 7.52 (s, 1H), 7.12 (m, 3H), 2.74 (m, 4H), 1.60 (m, 4H), 1.28 (m, 12H), 0.84 (m, 6H). ^{13}C NMR (300 MHz, $CDCl_3$) δ ppm 178.6, 177.5, 155.3, 138.8, 129.9, 129.5, 127.6, 124.9, 123.9, 123.4, 122.4, 121.3, 120.2, 117.9, 112.5, 28.2, 27.1, 26.8, 25.8, 25.0, 24.6, 18.0, 17.7, 9.5. HRMS (CI, 70 ev) *m/z*: [$(M+H)^+$] 748.1954 g mol^{-1} e^{-1} and [$(M–C_{29}H_{33}S_4O)^+$] 221.0 g mol^{-1} e^{-1}; calculated: 747.72 g/mol ($C_{43}H_{41}NO_3S_4$).

2.2. Methods

UV–vis absorption spectra were recorded using a Beckman model DU-640B spectrophotometer. Steady state and time-resolved emission measurements were conducted with a FluoroLog-3 spectrofluorometer equipped with double-grating monochromators, a TBX single-photon-counting detector and a NanoLED laser source (λ_{ex} = 406 nm; half-height pulse width, $w_{1/2}$ = 195 ps). The intensity of the excitation light was controlled by placing selected reflection neutral-density filters in front of the laser. For recording the profile of the excitation pulse (i.e., the scatterer), we used aqueous solution of bovine serum albumin or nondairy creamer.

Stock solutions of T4–AQ and T4a (1–10 mM) in toluene or DMSO were prepared prior to each series of experiments. For the measurements, small amounts of stock solution were diluted 100- to 1000-fold with the solvent of interest.

We used dilute chromophore solutions (OD(λ_{ex}) < 0.20) for the fluorescence measurements to avoid self-absorption and re-emission. Stock solutions in toluene or DMSO were prepared. The samples were prepared by adding minute amounts of the stock solutions to the solvent of interest. The final concentrations of DMSO or toluene from the stock solutions in the samples were kept under ∼1%.

The experiments were conducted at room temperature using 1 cm quartz cuvette. Comparative measurements of aerated samples and samples purged with argon revealed that the presence of air does not cause detectable changes in the emission intensities and lifetimes.

The fluorescence quantum yields, Φ_f, were determined by comparing the integrated emission intensities of the samples with the integrated fluorescence of a reference sample with a known fluorescence quantum yield, Φ_{f0} [53,54]:

$$\Phi_f = \Phi_{f0} \frac{\int F(\lambda)d\lambda}{\int F_0(\lambda)d\lambda} \times \frac{1 - 10^{-A_0(\lambda_{ex})}}{1 - 10^{-A(\lambda_{ex})}} \times \frac{n^2}{n_0^2} \quad (1)$$

where $F(\lambda)$ is the fluorescence intensity at wavelength λ; $A(\lambda_{ex})$ is the absorbance at the excitation wavelength; n is the refractive index of the media; and the suffix "0" indicates the quantities for the reference sample used. For a reference sample we used a solution of 9-phenyl-10-methylacridinium (PF_6^- salt) in acetonitrile (Φ_{f0} = 0.063) [55,56].

The fluorescence decays were recorded at the emission maxima, $\lambda_f^{(max)} \sim 500$ nm (Table 1), and fitted to mono- and multi-exponential functions via a deconvolution algorithm. For obtaining the profile of the excitation pulse, we used aqueous solution of non-dairy creamer as a scatterer. While the values of χ^2 allowed for evaluation of the quality of the obtained fits, the Durbin–Watson parameters reflected the appropriateness of the functions used for the data fits [57]. For solvents with polarities similar to or higher than the polarity of chloroform, the decays obtained for T4–AQ followed the profile of the scatterer and could not be reliably fit to mono- or multi-exponential functions.

Femtosecond transient absorption experiments were conducted using a Clark-MXR 2010 laser system and an optical

Table 1
Photophysical properties of T4–AQ and T4a in various organic solvents that are not hydrogen-bond donors[a]

Solvent (ε, n)[b]	Compound	$\lambda_a^{(max)}$ (nm)	$\lambda_f^{(max)}$ (nm)	Φ_f	τ_f (ns)[c] ($\langle\tau_{S1}\rangle$ (ns))[c]	k_f[d] $\times 10^9$ (s^{-1})	k_{nd}[d] $\times 10^9$ (s^{-1})
Hexane	T4a	392	470	0.18	0.529 ± 0.041	0.34	1.6
(2.0, 1.38)	T4–AQ	391	487	0.20	0.527 ± 0.014	0.38	1.5
Tetrachloromethane	T4a	401	500	0.17	0.631 ± 0.053	0.27	1.3
(2.2, 1.46)	T4–AQ	394	496	0.16	0.596 ± 0.015	0.27	1.4
Toluene	T4a	394	506	0.18	0.522 ± 0.036 (0.42 ± 0.06)	0.34	1.6
(2.4, 1.50)	T4–AQ	402	501	0.11	0.785 ± 0.016 (0.80 ± 0.09)	0.14	1.1
Chloroform	T4a	404	505	0.13	0.474 ± 0.023 (0.37 ± 0.07)	0.27	1.8
(4.8, 1.45)	T4–AQ	394	–[e]	–[e]	–[e]	–[e]	–[f]
Ethylacetate	T4a	400	500	0.16	0.504 ± 0.037	0.32	1.7
(6.0, 1.37)	T4–AQ	391	–[e]	–[e]	–[e]	–[e]	–[f]
Tetrahydrofuran	T4a	406	501	0.18	0.558 ± 0.043	0.32	1.5
(7.5, 1.41)	T4–AQ	384	–[e]	–[e]	–[e]	–[e]	–[f]
Dichloromethane	T4a	395	513	0.16	0.540 ± 0.041 (0.40 ± 0.05)	0.30	1.6
(9.1, 1.44)	T4–AQ	400	–[e]	–[e]	–[e]	–[e]	–[f]
Acetone	T4a	387	499	0.14	0.581 ± 0.001	0.24	1.5
(22, 1.36)	T4–AQ	400	–[e]	–[e]	–[e]	–[e]	–[f]
Acetonitrile	T4a	386	498	0.16	0.631 ± 0.053 (0.48 ± 0.07)	0.25	1.3
(38, 1.34)	T4–AQ	400	–[e]	–[e]	–[e]	–[e]	–[f]

[a] Sample concentrations ~5 μM, $\lambda_{ex} = 406$ nm, half-height width of the excitation pulse, $w_{1/2} = 195$ ps.
[b] Solvent characteristics: ε is the relative dielectric constant and n is the index of refraction.
[c] Fluorescence decay lifetimes, τ_f, are obtained from single-exponential data fits to the time-resolved emission data; [61] the average singlet-decay lifetimes, $\langle\tau_{S1}\rangle$, are obtained from triple-exponential fits to the absorption, ΔA, decays of the singlet, S_1, transients of T4 [62].
[d] The radiative and non-radiative decay rate constants were calculated from the fluorescence quantum yields and the lifetimes: $k_f = \Phi_f/\tau_f$; $k_{nd} = (1 - \Phi_f)/\tau_f$.
[e] For these solvents, the emission of T4–AQ is practically completely quenched resulting in quantum yields of T4–AQ smaller than about 10^{-3}. In addition, the relatively broad excitation pulsewidth did not allow us to determine the lifetimes of T4–AQ. We can safely assume that $\tau^{(T4-AQ)}$ are shorter than ~20 ps.
[f] Assuming $\Phi_f{}^{(T4-AQ)} < 10^{-3}$ and $\tau_f{}^{(T4-AQ)} < 20$ ps, implies that $k_{nd}{}^{(T4-AQ)} > 5 \times 10^{10}$ s^{-1}.

detection system, Helios, provided by Ultrafast Systems [58]. The fundamental output of the Clark laser system (775 nm, 1 mJ/pulse, FWHM = 130 fs, 1 kHz repetition rate) was split into 95 and 5% for the pump and the probe pulses, respectively. The pump beam is passed through a second-harmonic generator and its power is attenuated to 5 μJ/pulse. The probe beam is passed through a delay line (experimental time window is 1.6 ns with a step resolution ≥ 7 fs) followed by a white-light generator. After passing through the sample, the probe-beam is analyzed with CCD spectrographs: Ocean Optics, S2000 UV–vis (425–800 nm) and/or Sensors Unlimited, SU-LDV-512LDB (750–1200 nm). Due to interference of the scatter from the fundamental wavelength (775 nm) with the spectrographs, data points between 750 and 800 nm were not collected for the transient spectra.

Nanosecond transient absorption measurements were conducted with a system using Nd-YAG laser equipped with a third-harmonic generator as an excitation source [59]. All transient-absorption experiments were conducted at room temperature.

3. Results and discussion

3.1. Preparation of the electron donor–acceptor dyad (T4–AQ)

Condensation of a bifunctional dithiophene with two thiophene derivatives yielded a tetrathiophene conjugate that was consequently derivatized with a carboxyl group (Scheme 1). The hexyl chains in the (3,3‴-dihexyl)-2,2′:5′,2″:5″,2‴ quaterthiophene-5-carboxylic acid (T4a) were introduced for improvement of its solubility in organic solvents. The electron donor–acceptor dyad, T4–AQ, was formed through amide coupling between aAQ and T4a with its carboxyl group activated as an acid chloride. We observed a relatively low yield (~20%) in the last step of the synthesis of T4–AQ. We believe that this inefficiency in the formation of the amide bond is due to the electron-donating character of the quaterthiophene

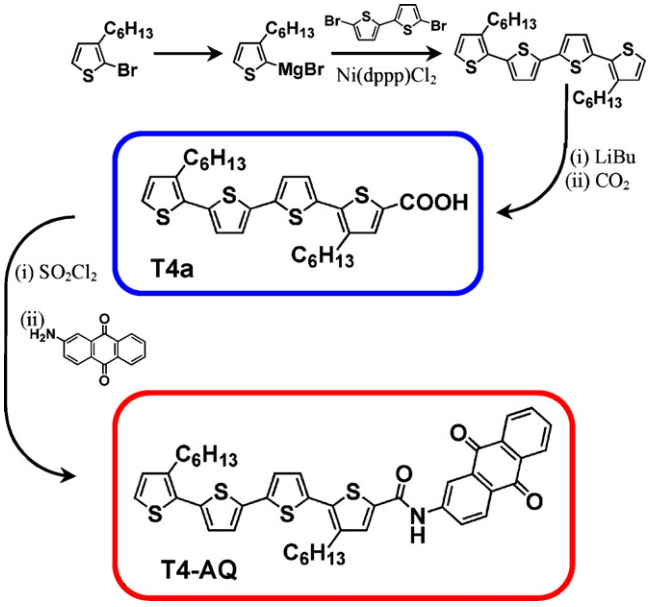

Scheme 1. Synthesis of the donor–acceptor dyad, T4–AQ.

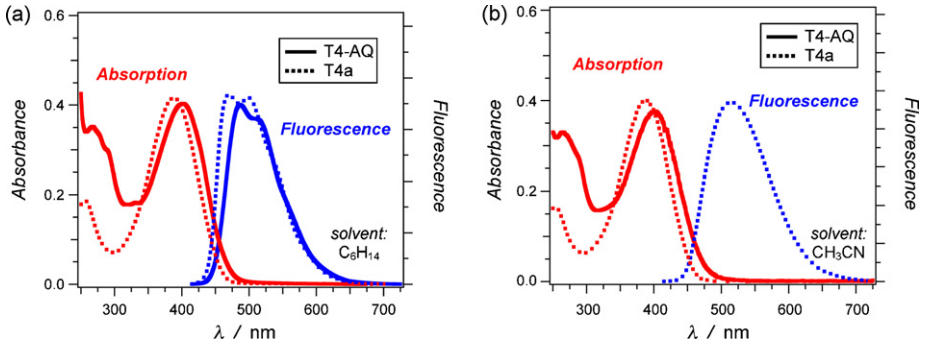

Fig. 1. Absorption and emission spectra of T4a and T4–AQ (10 μM) for: (a) hexane and (b) acetonitrile. (λ_{ex} = 405 nm).

that decreases the electrophilicity of the carbonyl carbon and the electron-withdrawing character of the anthraquione that decrease the nucleophilicity of the amine.

3.2. Absorption and emission properties of T4–AQ

A broad absorption band at about 400 nm, common for T4a and T4–AQ, is ascribed to the S_0–S_1 transition of T4 (Fig. 1). The peak at 255 nm, observed only for the dyad, is assigned to the lowest-energy allowed π–π* transitions of AQ [60].

For the various solvent media, excitation of T4a and T4–AQ at ~400 nm results in emission spectra identical for both compounds (Fig. 1). We ascribe the observed emission to the fluorescence of quaterthiophene moieties, produced from the locally singlet excited states of T4, ^{1}T4a* and ^{1}T4*–AQ.

Although AQ and T4 are separated only by an amide bond, the coupling between their π-electron systems is not strong enough to cause significant perturbation in the T4 absorption spectra. For the different solvents used, the wavelength maxima of the absorption and emission bands ($\lambda_a^{(max)}$ and $\lambda_f^{(max)}$, respectively) of T4–AQ did not manifest sovatochromism that correlates with the solvent polarity (Table 1), suggesting that the excited state, from which the emission occurs upon photoexcitation at ~400 nm, does not possess a charge-transfer character.

From the measured fluorescence quantum yields, Φ_f, and lifetimes, τ_f, [61] we calculated the rate constants of the non-radiative, k_{nd}, and radiative, k_f, decay processes for the photoexcited conjugates in various solvents (Table 1). The lifetime and the non-radiative decay rate constant of T4a do not manifest dependence on the solvent polarity (Table 1). The presence of AQ in the dyad, however, quenches the T4 fluorescence when in relatively polar media. For solvents with dielectric constant similar to or higher than the dielectric constant of chloroform, $\Phi_f^{(T4–AQ)}$ could not be reliably calculated because of the extremely low emission recorded for the dyad. Furthermore, the emission decays recorded for T4–AQ in media with increased polarity, followed the profile of the excitation laser pulse, suggesting emission lifetimes that were shorter than about 20 ps – which is the low limit for single-photon-counting measurements obtained with 200 ps excitation-pulse width (Fig. 2).

Our findings suggest that for polar and moderately polar solvents $k_{nd}^{(T4–AQ)} \gg k_{nd}^{(T4a)}$. For each of the non-polar solvents, however, the values of $k_{nd}^{(T4–AQ)}$ and $k_{nd}^{(T4a)}$ are similar within a factor of about 1.5 (Table 1). We ascribe the observed solvent-dependent quenching of the emission of quaterthiophene in the dyad to an intramolecular electron transfer from T4 to AQ.

3.3. Transient-absorption spectroscopy

To gain further understanding of the charge-transfer kinetics mediated by the dyad, we conducted femtosecond laser flash photolysis experiments with T4–AQ and T4a in four solvents

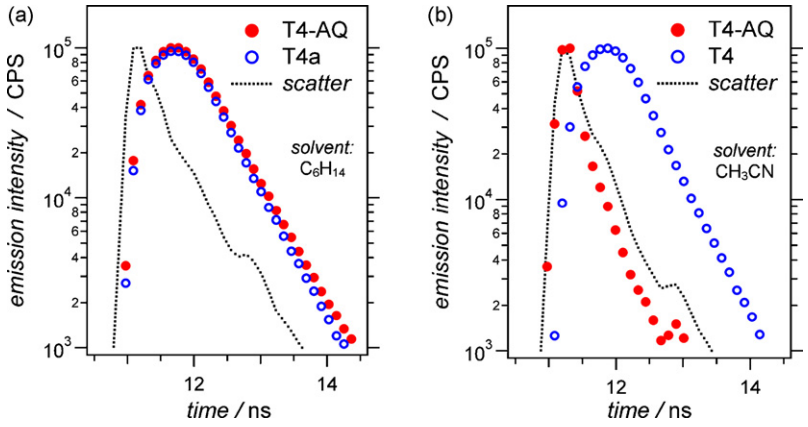

Fig. 2. Decays of the emission of T4a and T4–AQ dissolved in: (a) hexane and (b) acetonitrile. (Single photon counting: λ_{ex} = 406 nm, λ_{em} = 500 nm.)

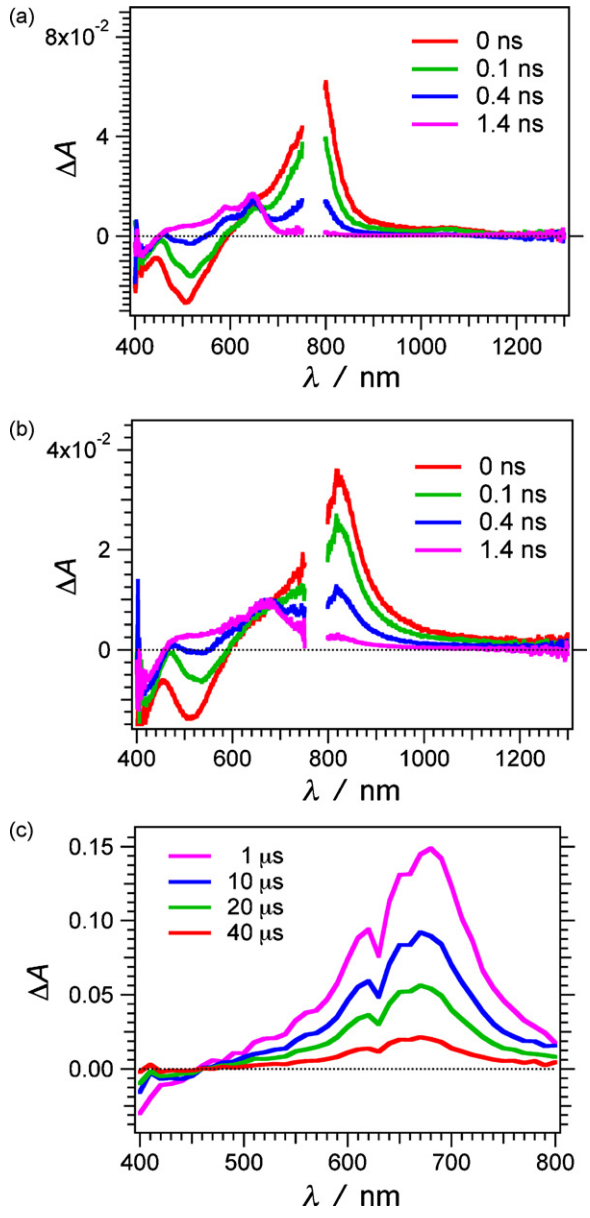

Fig. 3. Transient absorption spectra of: (a) T4a and (b and c) T4–AQ for toluene, recorded with (a and b) femtosecond (half-height pulse width, $w_{1/2} = 130$ fs, $\lambda_{ex} = 387$ nm) and (c) nanosecond ($w_{1/2} = 8$ ns, $\lambda_{ex} = 355$ nm) laser flash photolysis spectrometers. The singlet-excited quaterthiophene, ^{1}T4*, absorbs at (a) 800 nm and (b) 850 nm. In the picosecond and nanosecond spectra, the fluorescence from ^{1}T4* appears as a negative ΔA band at 510 nm. The long-lived triplet-excited quaterthiophene, ^{3}T4*, shows a broad absorption band between 550 and 750 nm.

with different polarities: toluene, chloroform, dichloromethane and acetonitrile.

For toluene, the transient spectra of T4–AQ and T4a closely resembled each other (Fig. 3), confirming that photoexcitation of T4–AQ in non-polar solvents does not initiate charge separation. The sharp absorption band observed for T4a and T4–AQ at about 800 nm is ascribed to the singlet excited state of the quaterthiophene, ^{1}T4* (Fig. 3). The absorption maximum of ^{1}T4*–AQ manifests about a 20 nm red shift in comparison with ^{1}T4a*, resembling the trend observed for ground-state absorption for toluene (Table 1). The lifetimes of the ^{1}T4*–AQ and ^{1}T4a* transients for toluene were about 0.5 ns, which is in a good agreement with the time-resolved emission results (Table 1).

In addition to the bleaching of the ground-state absorption at about 400 nm, we observed another negative band at about 500 nm, which is due to the fluorescence of T4 (Fig. 3). The relatively weak long-lived transient, spread between about 550 and 700 nm, is ascribed to the quaterthiophene triplet excited state, ^{3}T4* [47]. Nanosecond transient absorption measurements in the presence and absence of oxygen confirmed this assignment. While for deaerated samples the lifetime of the transient at

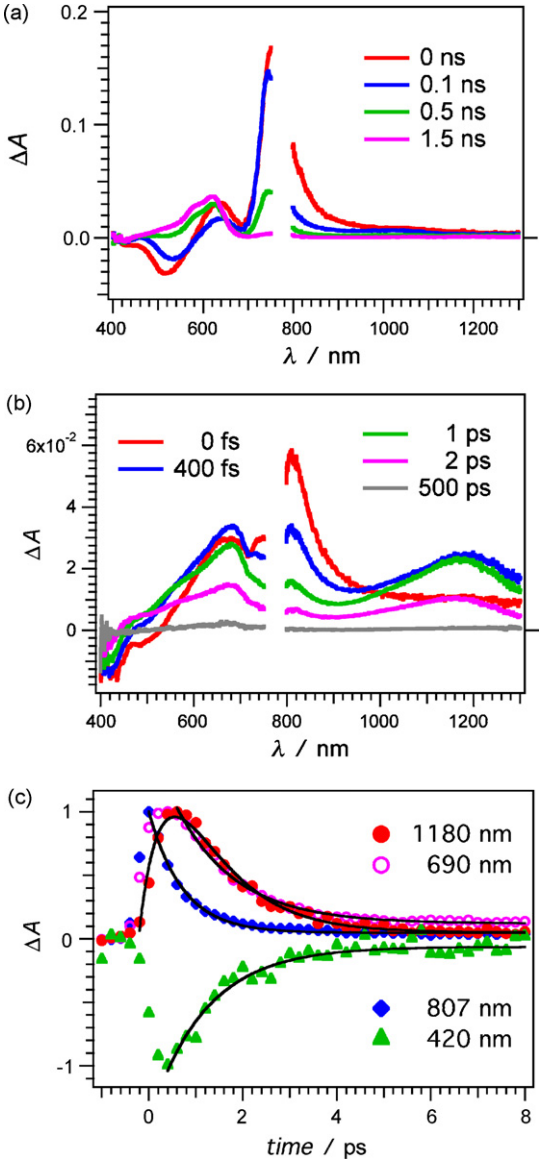

Fig. 4. Transient absorption spectra of: (a) T4a and (b) T4–AQ for acetonitrile. (c) Time-resolved decays for the T4–AQ transients, shown on (b): 807 nm – ^{1}T4* (singlet excited state); 420 nm – ^{1}T4 (bleach recovery of the T4 ground state); 1180 nm – $T4^{+\bullet}$ (oxidized quaterthiophene); 690 nm – $T4^{+\bullet}$ and $AQ^{-\bullet}$ (oxidized quaterthiophene and reduced anthraquinone). The decay at 690 nm and the bleach recovery at 420 nm do not completely reach zero values within the time span of the measurement because of the small amounts of triplet formation. The maxima of the decay data are normalized to $\Delta A = 1$. The gray curves represent the exponential data fits. (Half-height pulse width, $w_{1/2} = 130$ fs, $\lambda_{ex} = 387$ nm.)

600 nm is about 23 μs, in the presence of oxygen its lifetime shortens to about 0.21 μs.

For polar solvents, the transient spectra for T4–AQ and T4a are distinctly different. While the spectra of the photogenerated transients for T4a in acetonitrile and toluene closely resemble each other (Fig. 4a), the spectra for T4–AQ in acetonitrile show three distinct short-lived transients (Fig. 4b) [62]. In addition to the T4 singlet-excited-state, absorbing at 810 nm, we observed a broad band centered at 1180 nm, which we ascribe to the infrared absorption of the oxidized quaterthiophene, $T4^{+}$ [35,47,63]. The transient absorption band spread between about 500 and 700 nm is an overlap between the spectra of the two charge-transfer species. The visible absorption band of $T4^{+\bullet}$ peaks at 670 nm [63]. The principal absorption band of the singly reduced anthraquinone moiety, $AQ^{-\bullet}$, is situated around 530 nm [64] and it appears as a shoulder of the $T4^{+\bullet}$ absorption band (Fig. 4b).

The rise and decay times for the observed transients allowed us to quantify the charge-transfer kinetics for T4–AQ in acetonitrile. The decay time of the T4 singlet excited state, 0.7 ps, was identical with the rise time of the oxidized T4 transient monitored at 1180 nm (Fig. 4c). Therefore, the inverted times for the $^{1}T4^{*}$ decay and $T4^{+\bullet}$ rise allowed us to estimate the value of the photoinduced charge separation rate constant for T4–AQ in acetonitrile, $k_{CS} = 1.4 \times 10^{12}\ s^{-1}$ (Table 2).

The decay times of the charge-transfer transients, monitored at the infrared and the visible region, were identical, 1.3 ps. These decay times were in good agreement with the bleach-recovery time constant of the T4–AQ ground-state absorption, which was 1.2 ps, allowing us to estimate the charge-recombination rate constant, $k_{CR} = 7.7 \times 10^{11}\ s^{-1}$ (Table 2).

Similar kinetic analysis was conducted for T4–AQ in chloroform and dichloromethane (Table 2) [65]. Notably, the rates of the forward electron transfer were faster than the rates of the back electron transfer for the three relatively polar solvents.

Decrease in the solvent polarity slows down both the forward and back electron transfer. This effect is more pronounced for the charge-recombination than for the charge-separation processes: while the difference between k_{CS} for acetinitrile and chloroform is about seven-fold, the value of k_{CR} for acetonitrile is 55 times larger than the value of k_{CR} for chloroform (Table 2).

3.4. Electron-transfer kinetics

Through a semiclassical non-adiabatic approximation, the Marcus transition-state theory shows the relationship between the rate constant, k_{et}, and the driving force, $\Delta G^{(0)}_{et}$, of an electron-transfer process [15,66]:

$$k_{et} = \frac{2\pi}{\hbar}(H_{DA})^2 \frac{1}{\sqrt{2h\lambda k_B T}} \exp\left(-\frac{(\Delta G^{(0)}_{et} + \lambda)^2}{4\lambda k_B T}\right) \quad (2)$$

The Rehm–Weller equation allows us to estimate the driving force for photoinduced electron transfer from electrochemically and spectroscopically measurable quantities [33,67–72]:

$$\Delta G^{(0)}_{et} = F(E^{(0)}_{D^{+\bullet}/D} - E^{(0)}_{A/A^{-\bullet}}) - \mathcal{E}_{00} + \Delta G_S + W \quad (3)$$

Because of the relatively high polarity of the electrolyte solutions used for the electrochemical measurements, we approximated the expression for the Born solvation term, ΔG_S, by neglecting the values for the inverted dielectric constants of the media for the redox experiments [72]. Such approximation proved to be better than ascribing the dielectric constants of neat organic solvents to the dielectric values of the organic electrolyte solutions used for measuring the redox potentials of the donor and the acceptor.

The thermodynamic driving force, expressed in Eq. (3), represents the forward electron transfer, i.e., the photoinduced charge separation, $\Delta G^{(0)}_{CS}$, which is directly related to driving force for the consequent charge recombination, $\Delta G^{(0)}_{CR}$:

$$\Delta G^{(0)}_{CS} + \Delta G^{(0)}_{CR} = -\mathcal{E}_{00} \quad (4)$$

The calculated values of the driving force for the forward and back electron transfer for T4–AQ in various solvents show a strong dependence on the polarity of the solvent (Table 3). While for non-polar solvents, e.g., toluene, hexane and tetrachloromethane, the values of $\Delta G^{(0)}_{CS}$ are positive, for solvents with polarities similar to or larger than the polarity of chloroform, the values of $\Delta G^{(0)}_{CS}$ are negative. Furthermore, the increase in the solvent polarity results in more negative values for the charge-separation driving force (Table 3). Due to the lack of significant solvatochromic effects, the differences

Table 2
Time and rate constants of photoinduced charge separation and consequent charge recombination extracted from transient absorption data for T4–AQ in different solvents

Solvent	Charge separation		Charge recombination	
	τ (ps)	$k \times 10^{-11}(s^{-1})$	τ (ps)	$k \times 10^{-11}(s^{-1})$
Chloroform	4.7	2.1	73	0.14
Dichloromethane	1.2	8.3	15	0.67
Acetonitrile	0.70	14	1.3	7.7

Table 3
Calculated driving force of the intramolecular photoinduced charge separation, $\Delta G^{(0)}_{CS}$, and consequent charge recombination, $\Delta G^{(0)}_{CR}$, for T4–AQ in different solvents

Solvent	$\Delta G^{(0)}_{CS}$ (eV)[a]	$\Delta G^{(0)}_{CR}$ (eV)[b]	λ_{out} (eV)[c]
Hexane	0.20	−2.9	0.070
Tetrachloromethane	0.095	−2.8	0.051
Toluene	0.029	−2.7	0.062
Chloroform	−0.44	−2.3	0.60
Ethylacetate	−0.52	−2.2	0.81
Tetrahydrofuran	−0.60	−2.1	0.83
Dichloromethane	−0.65	−2.0	0.82
Acetone	−0.79	−1.9	1.1
Acetonitrile	−0.84	−1.9	1.2

[a] Calculated from Eq. (3) [71,72].
[b] Calculated from Eqs. (3) and (4) [71,72].
[c] The reorganization energy (λ in Eqs. (2) and (3)) can be represented as a sum of the inner and outer (or external) reorganization energies External reorganization energy, λ_{out}, is calculated from the continuum dielectric model: $\lambda_{out} = (\Delta e)^2(4\pi\varepsilon_0)^{-1}((2r_D)^{-1} + (2r_A)^{-1} - r^{-1})(n^{-2} - \varepsilon^{-1})$ [66,71].

in the estimated values for $\mathcal{E}_{00}$ for the various solvents do not exceed 0.15 eV. Therefore, the media dependence of the redox potentials of the charge-transfer species, introduced as ΔG_S, appears to be the principal reason for the dramatic dependence of the values of $\Delta G^{(0)}_{CS}$ and $\Delta G^{(0)}_{CR}$ on the solvent polarity [73].

The driving-force calculations are in a good agreement with the emission and transient-absorption results. Quenching of the quaterthiophene fluorescence of T4–AQ was observed for media providing favorable driving forces for the photoinduced charge transfer, i.e., for solvents resulting in $\Delta G^{(0)}_{CS} < 0$ (Table 1). Also, increase in the solvent polarity resulted in increase in the observed charge-separation rates (Table 2). Therefore, our calculations and experimental findings indicate that the solvent modulation of the electron-transfer properties of T4–AQ is caused by the stabilization of the charge-transfer state, $T4^{+\bullet}$–$AQ^{-\bullet}$, in media with increased polarity (Scheme 2). For solvents with polarities similar to or larger than the polarity of chloroform, the energy of the charge-transfer state lies below the energy of the locally-excited singlet state, ^{1}T4*–AQ, making electron transfer thermodynamically favorable upon excitation of the quaterthiophene moiety.

For all investigated solvents, $\Delta G^{(0)}_{CR}$ was more negative than $\Delta G^{(0)}_{CS}$ (Table 3), making the back electron transfer thermodynamically more favorable than the forward photoinduced electron transfer. The measured rate constants for charge separation, however, were about 2–15 times larger than the rate constants for charge recombination (Table 2). These findings suggest that the back charge-transfer processes observed for T4–AQ in the investigated solvent media occur under a regime situated in the Marcus inverted region.

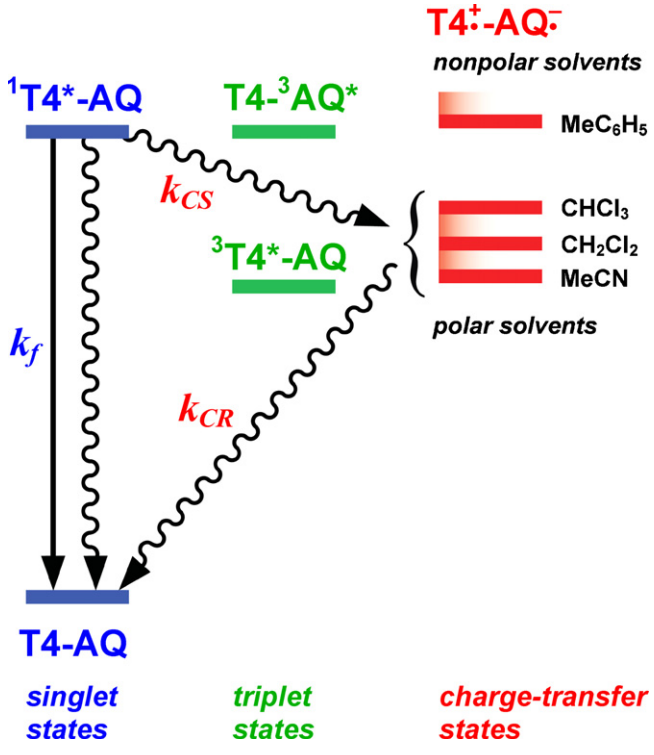

Scheme 2. Jablonski diagram for T4AQ in three different solvents: chloroform ($CHCl_3$), dichloromethane (CH_2Cl_2) and acetonitrile (MeCN).

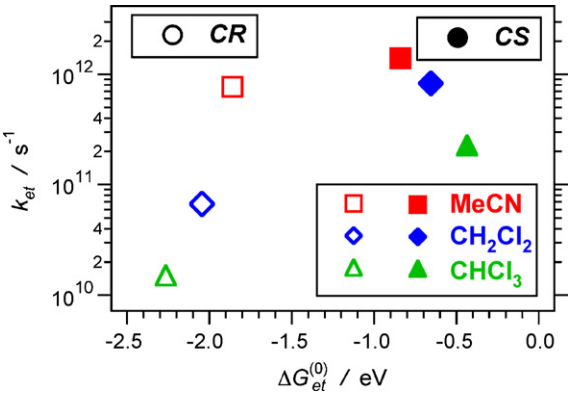

Fig. 5. Dependence of electron-transfer rate constants, k_{et}, obtained from transient-absorption measurements (Table 2), on the calculated electron-transfer driving force, $\Delta G^{(0)}_{et}$ (Eqs. (3) and (4), Table 3). (MeCN = acetonitrile, CH_2Cl_2 = dichloromethane and $CHCl_3$ = chloroform.).

Fig. 5 shows a dependence of the measured electron-transfer rate constants on the driving force that resembles a Marcus-like curve. We, however, abstain from fitting our data to Eq. (2) mainly because the reorganization energy, λ, differs for T4–AQ in the different solvent media (Table 3). Although we did not observe charge-transfer character in the steady-state spectra of T4–AQ (Fig. 1, Table 1), the non-adiabatic nature of Eq. (2) should be considered when quantifying a system, in which the donor–acceptor coupling is not necessarily weak. Furthermore, Eq. (2) does not take into account the nuclear tunneling that may result in increased charge-transfer rates [1].

The observed solvent modulation of the intramolecular charge-separation and charge-recombination rates for T4–AQ reflects the trends expected according to the semiclassical charge-transfer theory (Eq. (2)). Expectedly, decrease in the solvent polarity increases the energy of the charge-separation state (Scheme 2) and decreases the outer reorganization energy (Table 3). Therefore, for a system with $\Delta G^{(0)}_{CS} \ll \Delta G^{(0)}_{CR}$, lessening the polarity of the media will shift the charge-separation process toward the tip of the Marcus curve and the charge-recombination further into the inverted region, a phenomenon that at first glance may explain the larger solvent dependence observed for k_{CR} in comparison with k_{CS} (Table 2).

Other studies on the solvent dependence of the charge-transfer properties of dyads show k_{CR} exceeding k_{CS} up to several orders of magnitude [35,74–78]. As it has been pointed out, however, many of the reported long-lived photogenerated charge-separation species possess triplet character [1]. The T4 triplet state has lower energy than T4–AQ charge-transfer states (Scheme 2) and our transient-absorption data do not reveal involvement of triplet species in the charge-transfer processes. Indeed, the subpicosecond transient absorption spectroscopy that we employed in this study offered sufficient temporal resolution that allowed us to directly monitor the formation and the decay of the singlet locally excited state, ^{1}T4*–AQ, leading to the rise and the decay of the charge-transfer state, $T4^{+\bullet}$–$AQ^{-\bullet}$,

with concurrent disappearance and recovery of the ground state, T4–AQ (Fig. 4c).

4. Conclusions

We observed a strong dependence of the intramolecular charge-transfer properties of an electron donor–acceptor dyad on the solvent polarity. Alterations in the polarity of the media caused substantial changes in the energy level of the charge-transfer state of the dyad (Scheme 2), reflecting the changes in the driving force of the electron-transfer processes (Table 3): e.g., more than 1 eV difference between the values of the driving force for hexane and acetonitrile. This modulation of the Frank–Condon component of the electron-transfer rate constant (Eq. (2)) results in suppression of the photoinduced charge separation for the dyad in non-polar media (Fig. 3), while for polar and moderately polar solvents, the charge transfer processes occur in the femto- and picosecond time domains (Fig. 4).

The driving force of the back electron transfer for the solvents, in which charge separation was observed, varies between −1.9 and −2.3 eV, placing the charge recombination processes in the Marcus inverted region. As a result, for the investigated solvents, the charge-recombination rates were slower than the corresponding rates of photoinduced charge separation, which illustrates a type of charge-transfer kinetics that is essential for light-energy-conversion systems. This study shows an example for achieving such kinetic behavior by using media polarity for tuning the driving force and the reorganization energy of the charge-transfer processes.

Acknowledgements

The work described herein was supported by the UC Energy Institute and Office of the Basic Energy Sciences of the US Department of Energy. We extend our gratitude to the National Science Foundation for the REU funding (BRITE@UCR) that provided part of the support for A.F. We also would like to thank Toyota Central R&D Labs., Inc., Aichi, Japan for the research grant for enabling the stay of T.K. at Notre Dame. This is contribution No. NDRL 4744 from the Notre Dame Radiation Laboratory.

References

[1] J.W. Verhoeven, H.J. van Ramesdonk, M.M. Groeneveld, A.C. Benniston, A. Harriman, ChemPhysChem 6 (2005) 2251–2260.
[2] T.V. Duncan, T. Ishizuka, M.J. Therien, J. Am. Chem. Soc. 129 (2007) 9691–9703.
[3] M. Di Valentin, A. Bisol, G. Agostini, A.L. Moore, T.A. Moore, D. Gust, R.E. Palacios, S.L. Gould, D. Carbonera, Mol. Phys. 104 (2006) 1595–1607.
[4] G. Jones II, L.N. Lu, J. Org. Chem. 63 (1998) 8938–8945.
[5] G. Jones II, V.I. Vullev, Org. Lett. 4 (2002) 4001–4004.
[6] A. Knorr, E. Galoppini, M.A. Fox, J. Phys. Org. Chem. 10 (1997) 484–498.
[7] M.A. Fox, E. Galoppini, J. Am. Chem. Soc. 119 (1997) 5277–5285.
[8] E. Galoppini, M.A. Fox, J. Am. Chem. Soc. 118 (1996) 2299–2300.
[9] T. Morita, S. Kimura, J. Am. Chem. Soc. 125 (2003) 8732–8733.
[10] S. Yasutomi, T. Morita, Y. Imanishi, S. Kimura, Science 304 (2004) 1944–1947.
[11] Y.-G.K. Shin, M.D. Newton, S.S. Isied, J. Am. Chem. Soc. 125 (2003) 3722–3732.
[12] G. Jones II, D. Yan, J. Hu, J. Wan, B. Xia, V.I. Vullev, J. Phys. Chem. B 111 (2007) 6921–6929.
[13] H.J. Wolff, D. Buerssner, U.E. Steiner, Pure Appl. Chem. 67 (1995) 167–174.
[14] E. Vauthey, D. Phillips, Chem. Phys. 147 (1990) 421–430.
[15] R.A. Marcus, N. Sutin, Biochim. Biophys. Acta, Rev. Bioenerg. 811 (1985) 265–322.
[16] It is a common understanding that the charge-transfer driving force is not literally force: it represents the free-energy difference, ΔG, between the final and the initial state. Increase in the driving force corresponds to shifting ΔG toward more negative values.
[17] C. Serpa, P.J.S. Gomes, L.G. Arnaut, S.J. Formosinho, J. Pina, J. Seixas de Melo, Chem.—Eur. J. 12 (2006) 5014–5023.
[18] S.J. Formosinho, L.G. Arnaut, R. Fausto, Prog. React. Kinet. 23 (1998) 1–90.
[19] L.G. Arnaut, S.J. Formosinho, THEOCHEM 79 (1991) 209–230.
[20] S. Hotta, Y. Ichino, Y. Yoshida, Electronic and Optical Properties of Conjugated Molecular Systems in Condensed Phases, 2003, pp. 615–635.
[21] D. Fichou, J. Mater. Chem. 10 (2000) 571–588.
[22] A.R. Murphy, J.M.J. Frechet, Chem. Rev. 107 (2007) 1066–1096.
[23] J. Locklin, M. Roberts, S. Mannsfeld, Z. Bao, Polym. Rev. 46 (2006) 79–101.
[24] D.K. James, J.M. Tour, Top. Curr. Chem. 257 (2005) 33–62.
[25] I.F. Perepichka, D.F. Perepichka, H. Meng, F. Wudl, Adv. Mater. 17 (2005) 2281–2305.
[26] G. Barbarella, Electronic and Optical Properties of Conjugated Molecular Systems in Condensed Phases, 2003, pp. 79–97.
[27] S. Hotta, Trans. Mater. Res. Soc. Jpn. 29 (2004) 985–990.
[28] T. Otsubo, Y. Aso, K. Takimiya, J. Mater. Chem. 12 (2002) 2565–2575.
[29] T. Otsubo, Y. Aso, K. Takimiya, Pure Appl. Chem. 77 (2005) 2003–2010.
[30] S. Chaudhary, H. Lu, A.M. Mueller, C.J. Bardeen, M. Ozkan, Nano Lett. 7 (2007) 1973–1979.
[31] F. Zhang, M. Ceder, O. Inganaes, Adv. Mater. 19 (2007) 1835–1838.
[32] K. Kim, J. Liu, M.A.G. Namboothiry, D.L. Carroll, Appl. Phys. Lett. 90 (2007) 163511/163511–163511/163513.
[33] H. Kanato, K. Takimiya, T. Otsubo, Y. Aso, T. Nakamura, Y. Araki, O. Ito, J. Org. Chem. 69 (2004) 7183–7189.
[34] A. Yassar, C. Videlot, A. Jaafari, Solar Energy Mater. Solar Cells 90 (2006) 916–922.
[35] Y. Oseki, M. Fujitsuka, D.W. Cho, A. Sugimoto, S. Tojo, T. Majima, J. Phys. Chem. B 109 (2005) 19257–19262.
[36] J. Cremer, P. Baeuerle, Eur. J. Org. Chem. (2005) 3715–3723.
[37] M.M.M. Raposo, A.M.C. Fonseca, G. Kirsch, Tetrahedron 60 (2004) 4071–4078.
[38] P.A. Van Hal, E.H.A. Beckers, S.C.J. Meskers, R.A.J. Janssen, B. Jousselme, P. Blanchard, J. Roncali, Chem.—Eur. J. 8 (2002) 5415–5429.
[39] T. Nishizawa, K. Tajima, K. Hashimoto, J. Mater. Chem. 17 (2007) 2440–2445.
[40] F. Wuerthner, M.S. Vollmer, F. Effenberger, P. Emele, D.U. Meyer, H. Port, H.C. Wolf, J. Am. Chem. Soc. 117 (1995) 8090–8099.
[41] D. Hirayama, K. Takimiya, Y. Aso, T. Otsubo, T. Hasobe, H. Yamada, H. Imahori, S. Fukuzumi, Y. Sakata, J. Am. Chem. Soc. 124 (2002) 532–533.
[42] S. Knorr, A. Grupp, M. Mehring, G. Grube, F. Effenberger, J. Chem. Phys. 110 (1999) 3502–3508.
[43] N. Mataga, H. Chosrowjan, S. Taniguchi, J. Photochem. Photobiol. C: Photochem. Rev. 6 (2005) 37–79.
[44] T.L. Netzel, Tetrahedron 63 (2007) 3491–3514.
[45] C. Reichardt, Pure Appl. Chem. 76 (2004) 1903–1919.
[46] E. Vauthey, J. Photochem. Photobiol. A: Chem. 179 (2006) 1–12.
[47] K. Matsumoto, M. Fujitsuka, T. Sato, S. Onodera, O. Ito, J. Phys. Chem. B 104 (2000) 11632–11638.
[48] J.S. de Melo, L.M. Silva, L.G. Arnaut, R.S. Becker, J. Chem. Phys. 111 (1999) 5427–5433.

[49] H. Higuchi, T. Nakayama, H. Koyama, J. Ojima, T. Wada, H. Sasabe, Bull. Chem. Soc. Jpn. 68 (1995) 2363–2377.
[50] K. Tanaka, K. Takimiya, T. Otsubo, K. Kawabuchi, S. Kajihara, Y. Harima, Chem. Lett. 35 (2006) 592–593.
[51] H. Higuchi, Y. Uraki, H. Yokota, H. Koyama, J. Ojima, T. Wada, H. Sasabe, Bull. Chem. Soc. Jpn. 71 (1998) 483–495.
[52] J. Kagan, S.K. Arora, A. Ustunol, J. Org. Chem. 48 (1983) 4076–4078.
[53] J.N. Demas, G.A. Crosby, J. Phys. Chem. 75 (1971) 991–1024.
[54] B. Valeur, Molecular Fluorescence, Principles and Applications, Wiley-VCH, 2002, p. 53.
[55] G. Jones II, D.-X. Yan, S.R. Greenfield, D.J. Gosztola, M.R. Wasielewski, J. Phys. Chem. A 101 (1997) 4939–4942.
[56] H. van Willigen, G. Jones II, M.S. Farahat, J. Phys. Chem. 100 (1996) 3312–3316.
[57] D.F. Eaton, Pure Appl. Chem. 62 (1990) 1631–1648.
[58] K. Takechi, P.K. Sudeep, P.V. Kamat, J. Phys. Chem. B 110 (2006) 16169–16173.
[59] V.I. Vullev, G. Jones II, J. Appl. Sci. 5 (2005) 517–526.
[60] A. Kuboyama, S. Matsuzaki, H. Takagi, H. Arano, Bull. Chem. Soc. Jpn. 47 (1974) 1604–1607.
[61] The fluorescence lifetimes presented in Table 1 are obtained from reasonably good data fits to a monoexponential function as expected from the linear time-dependence of the logarithm of the emission intensity (Fig. 2). Subpicosecond transient-absorption measurements, however, indicate that the decays of T4 singlet excited state have multi-exponential character, which are best fit to a triexponential function. For all solvents, two of the lifetimes obtained from the triexponential fits of the transient absorption decays were shorter than about 200 ps. Therefore, they could not be clearly resolved with the single-photon-counting technique. The Durbin-Watson parameters, DW, for monoexponential fits of the emission decays of T4a for hexane, tetrachloromethane, toluene, chloroform, ethylacetate, tetrahydrofuran, dichloromethane, acetone and acetonitrile were, respectively, 1.2, 0.88, 1.1, 0.76, 0.92, 0.97, 1.0, 1.1 and 1.1. For the same solvents, pentaexponential fits yielded DW = 1.7, 1.7, 1.8, 1.5, 1.8, 2.0, 1.4, 1.9 and 1.8. Despite the clear improvement of DW for multi-exponential fits, we chose to work with the data obtained from the monoexponential analyses because we do not believe that all of the obtained lifetimes from the mutiexponential emission-decay fits possess true physical meaning for the properties of the system. For example, each multi-exponential emission-decay fit contains negative terms, characteristic of fluorescence rise with time constants in the order of tens or hundreds picoseconds. Concurrently, transient absorption data show that the T4 singlet absorption and the bleach due to the T4 fluorescence appear within the 130 fs laser pulse (Figs. 3 and 4). This discrepancy leads us to believe that the fluorescence rises observed in the time-resolved emission data and depicted by the multi-exponential fits are artifact of the measurements, rather than characteristic of the studied systems.
[62] For T4–AQ when photoinduced charge transfer occurs, the decays of the ^{1}T4* transients exhibit monoexponential character with lifetimes corresponding to the rise times for the charge-transfer species (Table 2). For T4–AQ in non-polar solvents and T4a, i.e., when charge transfer cannot be photoinitiated, however, the decays of the ^{1}T4* absorption could be reliably fit to multi-exponential functions with minimum of three components. The following singlet-excited-state lifetimes (with corresponding normalized pre-exponential factors), τ_{S1i} (α_i), were obtained for T4a: 0.022 ns (0.06), 0.18 ns (0.60) and 0.55 ns (0.34) for toluene (DW = 2.4); 0.0072 ns (0.49), 0.11 ns (0.24), 0.44 ns (0.27) for chloroform (DW = 2.3); 0.0031 ns (0.52), 0.089 ns (0.30), 0.50 ns (0.18) for dichloromethane (DW = 2.2); and 0.0015 ns (0.46), 0.11 ns (0.33), 0.59 ns (0.21) for acetnitrile (DW = 2.5). For T4–AQ in toluene, τ_{S1i} (α_i), were: 0.14 ns (0.37), 0.37 ns (0.35), 1.1 ns (0.28) (DW = 2.5). The average transient decay lifetimes were calculated, $\langle\tau_{S1}\rangle = (\Sigma\alpha_i\ \tau_{S1i}{}^2)/(\Sigma\alpha_i\tau_{S1i})$, and presented in Table 1. The multi-exponential nature of the ^{1}T4* transient decays can be ascribed to the conformer population of T4. The rotation around the carbon-carbon bonds connecting the thiophene rings is restricted due to partial π-conjugation. Should the energy barriers between the various cis and trans conformers are larger than the thermal energy, k_BT, which is about 0.05 eV for room temperature, the transition rates between the T4 conformations will be slow enough to yield multiple lifetimes measurable in the subnanosecond time domain. We believe that the rate constants of charge-separation from the locally excited states of the different T4 conformers are similar in values, resulting in monoexponential decays of the ^{1}T4*–AQ transients in relatively polar solvent media.
[63] S. Samori, M. Hara, S. Tojo, M. Fujitsuka, S.-W. Yang, A. Elangovan, T.-I. Ho, T. Majima, J. Phys. Chem. B 109 (2005) 11735–11742.
[64] H. Gorner, Photochem. Photobiol. 77 (2003) 171–179.
[65] Because the visible region of the absorption spectra of the charge-transfer transients (500–650 nm) overlaps with the T4 and AQ triplet transient absorption, as well as with the T4 emission, we determined that it is significantly more reliable to extract the charge-transfer kinetic data from the IR region of the absorption spectrum of the T4 radical-cation (i.e., 1180 nm).
[66] In Eq. (2), H_{DA} is the transition-state Hamiltonian, representing the coupling between the donor and the acceptor; $\hbar = h/2\pi$, where $h = 4.136 \times 10^{-15}$ eV s is the Planck's constant; $k_B = 8.617 \times 10^{-5}$ eV K^{-1} is the Boltzmann constant,; T is the temperature in K; and λ is the reorganization energy.
[67] D. Rehm, A. Weller, Isr. J. Chem. 8 (1970) 259–271.
[68] B. Keita, I. Kawenoki, J. Kossanyi, L. Nadjo, J. Electroanal. Chem. Interfacial Electrochem. 145 (1983) 311–323.
[69] S.L. Mecklenburg, D.G. McCafferty, J.R. Schoonover, B.M. Peek, B.W. Erickson, T.J. Meyer, Inorg. Chem. 33 (1994) 2974–2983.
[70] L. Jannelli, A. Lopez, S. Saiello, J. Chem. Eng. Data 28 (1983) 169–173.
[71] In Eq. (3), $E^{(0)}_{D^{+\bullet}/D}$ and $E^{(0)}_{A/A^{-\bullet}}$ are the standard oxidation potential of the donor and reduction potential of the acceptor, respectively (the single-electron reduction potential for AQ in acetonitrile is −0.85 V vs. SCE, and the oxidation potential for T4 in benzonitrile is 0.95 V vs. SCE); F is the Faraday constant, which is the electric charges in one mol of electrons or in a single electron, depending on the units for energy in the equation; $\mathcal{E}_{00}$ is the zero-to-zero energy of the principal chromophore that for T4 is about 2.7 eV and has very small solvent dependence: i.e., ±0.1 eV for the solvents used in this study; ΔG_S is the correction term for ion solvation, derived from the Born equation: $\Delta G_S = e^2(r_D{}^{-1}(\varepsilon^{-1} - \varepsilon_D{}^{-1}) + r_A{}^{-1}(\varepsilon^{-1} - \varepsilon_A{}^{-1}))(8\pi\varepsilon_0)^{-1}$; and the Coulombic term, W, for non-charged donor and acceptor is $W = -e^2(4\pi\varepsilon_0\varepsilon r)^{-1}$. In addition, $\varepsilon_0 = 5.526 \times 10^{-3}$ V^{-1} Å^{-1} is the dielectric permeability of vacuum; ε is the relative dielectric constant of the media used for the charge-transfer measurements; ε_D and ε_A are the dielectric constants of the media used for measuring the redox potentials of the donor, T4, and the acceptor, AQ, respectively; $r = 12$ Å is the center-to-center throughspace donor–acceptor distance; $r_D = 7$ Å and $r_A = 3$ Å are the average radii of the donor and the acceptor, respectively.
[72] 0.1 M salt solutions in organic solvents were used for measuring the redox potentials of T4 and AQ. Because our measurements indicate that the dielectric constants of these salt solutions, i.e., ε_D and ε_A, are significantly higher than the dielectric constants of the neat organic solvents composing the solutions, for the solvents used for charge-transfer measurements in this study, $\varepsilon^{-1} \gg \varepsilon_D{}^{-1}$ and $\varepsilon^{-1} \gg \varepsilon_A{}^{-1}$. Therefore, the Born correction term in Eq. (3) can be approximated to a simplified expression that does not include ε_D and ε_A: $\Delta G_S \approx e^2((r_D\varepsilon)^{-1} + (r_A\varepsilon)^{-1})(8\pi\varepsilon_0)^{-1}$. The values for $\Delta G^{(0)}_{CS}$ and $\Delta G^{(0)}_{CR}$ presented in Table 3 were calculated using this approximate expression for ΔG_S. Alternatively, using the extended expression for ΔG_S, in which the values for ε_D and ε_A are the values of the dielectric constants of the corresponding neat organic solvents, decreased the values of $\Delta G^{(0)}_{CS}$ with about 0.1 eV and yielded favorable driving forces for the photoinduced charge separation for T4–AQ in toluene and tetrachloromethane. Our experimental results, however, did not support such calculated findings. Therefore, ε_D and ε_A cannot assume the values of the dielectric constants of pure benzonitril and acetonitril, respectively, in the calculation of ΔG_S.
[73] A decrease in the dielectric constant of the media leads to more negative values for the Coulombic term, W, and to more positive values of the Born term, ΔG_S, in Eq. (3). For T4–AQ, the rate of increase in ΔG_S is faster than the rate of decrease in W, resulting in more positive driving force (i.e., destabilization of the charge-transfer state for

non-charged donor and acceptor) with decrease in the media dielectric constant.
[74] M. Fujitsuka, N. Tsuboya, R. Hamasaki, M. Ito, S. Onodera, O. Ito, Y. Yamamoto, J. Phys. Chem. A 107 (2003) 1452–1458.
[75] H. Imahori, M.E. El-Khouly, M. Fujitsuka, O. Ito, Y. Sakata, S. Fukuzumi, J. Phys. Chem. A 105 (2001) 325–332.
[76] M. Fujitsuka, O. Ito, T. Yamashiro, Y. Aso, T. Otsubo, J. Phys. Chem. A 104 (2000) 4876–4881.
[77] K. Ohkubo, H. Kotani, J. Shao, Z. Ou, K.M. Kadish, G. Li, R.K. Pandey, M. Fujitsuka, O. Ito, H. Imahori, S. Fukuzumi, Angew. Chem. Int. Ed. 43 (2004) 853–856.
[78] S. Fukuzumi, H. Kotani, K. Ohkubo, S. Ogo, N.V. Tkachenko, H. Lemmetyinen, J. Am. Chem. Soc. 126 (2004) 1600–1601.